Field Theory of Electromagnetic Brain Activity

V. K. Jirsa and H. Haken
Institute for Theoretical Physics and Synergetics, University of Stuttgart, Pfaffenwaldring 57/4, 70550 Stuttgart, Germany
(Received 7 February 1996)

A semiquantitative nonlinear field theory of the brain is presented derived from the quasimicroscopic conversion properties of neural populations. Realistic anatomical connectivity conditions like long range excitation and short range inhibition are used. Predictions of our field equation are checked against experimental MEG results. [S0031-9007(96)00748-X]

PACS numbers: 87.10.+e

The brain is considered as a complex, physical, and open system that exhibits spatiotemporal behavior at various time and length scales. A necessary condition for this pattern forming character of the brain is a nonlinear dynamics and a spatial interconnection of its elements, the neurons. The functional behavior of the brain is encoded in these spatiotemporal structures and can, at least partly, be extracted from the dynamics of the macroscopic quantities measured by the EEG and MEG. According to synergetics [1], this extraction contains all the relevant information about the spatiotemporal behavior of the brain and has, in general, a small number of degrees of freedom. This idea has been formalized to the *order parameter concept* based on circular causality: The order parameters are determined and created by the cooperation of microscopic quantities, but at the same time the order parameters govern the behavior of the whole system. Based on this approach phenomenological models were set up in the past for different experiments in order to find evolution equations that describe the experimentally observed macroscopic dynamics [2].

The purpose of this Letter is twofold: First, we derive a nonlinear partial differential equation from simple properties of neural populations. This field equation governs the dynamics of the macroscopic quantities measured by EEG and MEG. Second, with respect to a particular MEG experiment by Kelso *et al.* [3] we discuss the obtained field equation analytically and numerically and prove that it reproduces the experimentally observed phenomena. An explicit derivation and discussion of the field equation will be published elsewhere.

Single neurons have two main state variables: (1) Dendritic currents are generated by active synapses that serve as current sources causing the *waves* of extracellular fields. These waves mainly correspond to the quantities measured by EEG and MEG [4]. (2) Action potentials are generated at the somas of neurons and correspond to *pulses*. See [5] for a detailed discussion of these quantities and their experimental measurements. The conversion of pulses to current amplitude occurs at synapses, the dendritic wave amplitude is converted to a pulse frequency at the somas. In contrast to single neurons the pulse-to-wave conversion in neural ensembles is constrained to a linear small-signal range, whereas the wave-to-pulse conversion shows a sigmoidal behavior [4]. These two conversion operations are shown in Fig. 1.

The field variables $\psi_e(x,t)$ and $\psi_i(x,t)$ denote the deviations from a fixed physiological state of excitatory and inhibitory wave amplitude at location x at the time point t and $\psi_E(x,t)$, $\psi_I(x,t)$ the corresponding excitatory and inhibitory pulse amplitudes. We define the conversion operations by

$$\psi_j(x,t) = \int_\Gamma dX\, f_j(x,X) H_j(x,X,t)\,, \qquad (1)$$

where $j = e, i, E, I$. Here the function $H_j(x,X,t)$ represents the output of a conversion operation and $f_j(x,X)$ the corresponding distribution function depending on the spatial connectivity. The considered surface area of the brain is denoted by Γ. We utilize a hierarchy in time and spatial scales known from anatomy and physiology [6,7]. Synaptic delays, refractory times, and delays due to propagation along intracortical fibers (excitatory and inhibitory) are of the order of 1 msec, the neural membrane constant is in the 10 msec range [8]. Propagation along cortico-cortical fibers (only excitatory) causes delays of up to several 100 msec [8]. The spatial range of connectivity

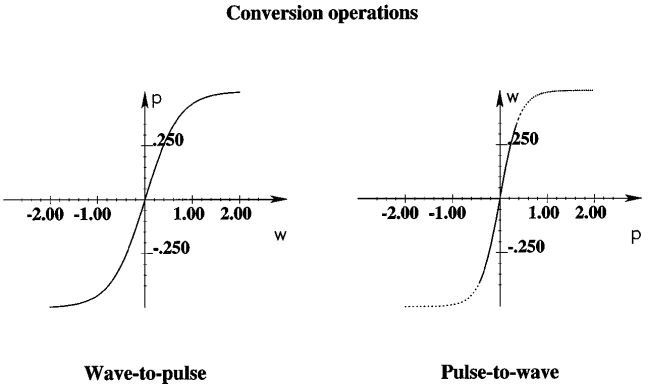

FIG. 1. On the left the wave-to-pulse conversion operation in neural ensembles is shown, on the right the same situation for the pulse-to-wave conversion.

 0031-9007/96/77(5)/960(4)$10.00

is for intracortical fibers about 0.1 cm and for corticocortical fibers 1 to 20 cm [5,6]. Cortical propagation velocities are in the range of 1 m/sec [7]. The time scale we want to consider here is in the range of 100 msec, the spatial scale in the range of several cm. Excitatory neurons have only excitatory synapses, inhibitory neurons only inhibitory synapses [6]. External input is realized such that afferent fibers make synaptic connections. These facts lead to the following relations between conversion output and pulse amplitudes:

$$H_e(x,X,t) = S[\psi_E(X,t- \mid x - X \mid /v)] \approx a_e \psi_E(X,t- \mid x - X \mid /v), \quad (2)$$

$$H_i(x,X,t) = S[\psi_I(X,t- \mid x - X \mid /v)] \approx a_i \psi_I(X,t- \mid x - X \mid /v), \quad (3)$$

and between conversion output and wave amplitudes

$$H_E(x,X,t) = S_e[\psi_e(X,t- \mid x - X \mid /v) - \psi_i(X,t- \mid x - X \mid /v) + p_e(X,t- \mid x - X \mid /v)], \quad (4)$$

$$H_I(x,X,t) = S_i[\psi_e(X,t- \mid x - X \mid /v) - \psi_i(X,t- \mid x - X \mid /v) + p_i(X,t- \mid x - X \mid /v)]. \quad (5)$$

Here a_e, a_i are constant parameters, v the velocity, $p_j(X,t)$ external input, and S, S_j the sigmoid functions of a class j ensemble. The distribution functions $f_E(x,X)$ and $f_I(x,X)$ are of short range and can be assumed to be δ functions. Inserting these into (1) we obtain

$$\psi_E(x,t) = \int_\Gamma dX\, \delta(x - X) H_E(x,X,t) = H_E(x,t) = S_e[\psi_e(x,t) - \psi_i(x,t) + p_e(x,t)], \quad (6)$$

$$\psi_I(x,t) = \int_\Gamma dX\, \delta(x - X) H_I(x,X,t) = H_I(x,t) = S_i[\psi_e(x,t) - \psi_i(x,t) + p_i(x,t)]. \quad (7)$$

In order to obtain the dynamics of the wave amplitudes $\psi_j(x,t)$ with $j = e,i$ we insert (2) and (3) into (1) and obtain

$$\psi_e(x,t) = \int_\Gamma dX\, f_e(x,X) H_e(x,X,t) = a_e \int_\Gamma dX\, f_e(x,X) \psi_E(X,t- \mid x - X \mid /v), \quad (8)$$

$$\psi_i(x,t) = \int_\Gamma dX\, f_i(x,X) H_i(x,X,t) = a_i \int_\Gamma dX\, f_i(x,X) \psi_I(X,t- \mid x - X \mid /v). \quad (9)$$

Inserting (6) into (8) and (7) into (9) the system reads

$$\psi_j(x,t) = a_j \int_\Gamma dX f_j(x,X) S_j[\psi_e(X,t- \mid x - X \mid /v) - \psi_i(X,t- \mid x - X \mid /v) + p_j(X,t- \mid x - X \mid /v)], \quad (10)$$

with $j = e,i$. In its linearized form this set of integral equations corresponds to the model equations by Nunez [9] and is discussed in [5]. We assume the connectivity functions to be of the following form:

$$f_j(x,X) = (2\sigma_j)^{-1} \exp(- \mid x - X \mid /\sigma_j), \quad (11)$$

with $j = e,i$. Here the spatial range of the distribution of the fibers defines a hierarchy in time scales on which $\psi_e(x,t)$ and $\psi_i(x,t)$ operate. Taking into account that intracortical fibers are only local the connectivity function $f_i(x,X)$ reduces to $\delta(x - X)$ in the short range limit. Inserting this into (10) with $j = i$ the inhibitory wave amplitude $\psi_i(x,t)$ becomes

$$\psi_i(x,t) = a_i S_i[\psi_e(x,t) - \psi_i(x,t) + p_i(x,t)]. \quad (12)$$

Taking only linear contributions of (12) into account we obtain the following behavior of the inhibitory wave amplitude:

$$\psi_i(x,t) \approx \frac{a_i \alpha_i}{1 + a_i \alpha_i} [\psi_e(x,t) + p_i(x,t)]. \quad (13)$$

Here the dynamics of $\psi_i(x,t)$ is expressed in terms of the leading order of the slowly varying field variables $\psi_e(x,t)$ and $p_i(x,t)$, which means that on this time scale the intrinsic dynamics of $\psi_i(x,t)$ is negligible. The higher order contributions of these quantities cause small modifications of the corresponding parameters and are neglected here. Inserting (13) into (10), we readily obtain a description in terms of the slow field variable $\psi_e(x,t)$ and the modified external input now denoted by $p(x,t)$,

$$\psi_e(x,t) = a_e \int_\Gamma dX\, f_e(x - X) \times S_e[\tilde{\rho} \psi_e(X,t- \mid x - X \mid /v) + p(X,t- \mid x - X \mid /v)], \quad (14)$$

where $\tilde{\rho}$ is a modified density due to the elimination of $\psi_i(x,t)$. Using the method of Green's functions we can rewrite the above integral equations as a nonlinear partial differential equation for the field $\psi_e(x,t)$

$$\ddot{\psi}_e + (\omega_0^2 - v^2 \triangle) \psi_e + 2\omega_0 \dot{\psi}_e = \left(\omega_0^2 + \omega_0 \frac{\partial}{\partial t}\right) \times \rho(x,t), \quad (15)$$

with

$$\rho(x,t) = a_e S_e[\tilde{\rho}\,\psi_e(x,t) + p(x,t)] \approx a_e\{\alpha_e[\tilde{\rho}\,\psi_e(x,t) + p(x,t)] - \tfrac{4}{3}\alpha_e^3[\tilde{\rho}\,\psi_e(x,t) + p(x,t)]^3\}, \quad (16)$$

where $\triangle$ denotes the Laplacian. In (16) we performed a Taylor expansion around the inflection point of the sigmoid function which we assumed to be the logistic curve. Here α_e is the slope of the sigmoid function and $\omega_0 = v/\sigma_e$. Equation (15) represents the dynamics of the field $\psi_e(x,t)$ interacting with functional units $p(x,t)$ which are embedded as inhomogeneities in the neural sheet.

We now want to tackle the field equation (15) with respect to the brain-behavior experiment by Kelso *et al.* [3]. In this experiment a subject was exposed to acoustic stimuli and pressed a button in a syncopated motion. The stimulus frequency at the beginning was set to 1 Hz and was increased by 0.25 Hz after 10 stimulus repetitions up to 2.25 Hz. Around the frequency of 1.75 Hz the subject switched spontaneously to a synchronized motion. During this experiment the magnetic field data were recorded over the left parietotemporal cortex, mainly covering the motor and auditory areas. Detailed analyses of the experimental data [10] revealed that phase transition phenomena can also be observed in the spatiotemporal dynamics of the brain. In the pretransition region this dynamics is dominated by one spatial mode corresponding to one stationary order parameter state oscillating mainly with the stimulus frequency. At the critical frequency a transition occurs to a new order parameter state with a different spatial structure mainly oscillating with twice the stimulus frequency. In the pretransition region the relative phase between brain signals and acoustic stimulus is locked and bistable, which means that two stationary states corresponding to antiphase and in phase of the relative phase between brain and stimulus signal coexist. At the critical frequency a transition by π from antiphase into in phase is observed as in the relative phase between motor and stimulus signal. In the posttransition region a monostable situation corresponding to in phase is present.

We specify the external acoustic stimulus representing the periodic acoustic signal $p(x,t) = \beta_{\mathrm{st}}(x)\sin\Omega t$ and assume as a first approximation that the stimulus is localized via a global coupling $\beta_{\mathrm{st}}(x) \approx \beta_{\mathrm{st}} = \mathrm{const}$ in the neural sheet. Ω denotes the stimulus frequency, which represents the control parameter in the present case. Inserting these into (15) we obtain

$$\ddot{\psi}_e + (\Omega_0^2 - v^2\triangle)\psi_e + \gamma_0\dot{\psi}_e + A\psi_e^3 + B\psi_e^2\dot{\psi}_e + \sum_{i=1}^{4} K_i = 0, \quad (17)$$

where

$$\begin{aligned} K_1 &= \epsilon[2\Omega\sin 2\Omega t\,\psi_e - \cos 2\Omega t(\dot{\psi}_e + \tilde{\omega}_0\psi_e)], \\ K_2 &= C[\Omega\cos\Omega t\,\psi_e^2 + \sin\Omega t(2\psi_e\dot{\psi}_e + \omega_0\psi_e^2)], \\ K_3 &= D_1(\Omega\cos\Omega t + \omega_0\sin\Omega t) + D_2[\Omega\cos 3\Omega t + (\omega_0/3)\sin 3\Omega t], \\ K_4 &= \gamma_1\dot{\overline{\psi}}. \end{aligned} \quad (18)$$

Here K_1 represents a parametric excitation of the neural tissue with twice the stimulus frequency, K_2 a nonlinear term with a parametric coefficient oscillating with the stimulus frequency, and K_3 a linear periodic driving of the neural tissue with the frequencies Ω and 3Ω. The last term K_4 is obtained from considerations about the motor feedback loop which we treat here in a linear approximation: The finger is assumed to be a linearly damped oscillator driven by the motor signal $\overline{\psi}(t)$ which represents the average activity of the neural sheet in a first approximation. As a feedback the finger oscillator sends a sensory-motor signal K_4 to the neural field ψ_e. Equation (17) determines the dynamics of a field containing linear and nonlinear damping terms, if $\gamma_0, B > 0$, and an amplitude dependent frequency. The most prominent feature of the above equations is the parametric excitation of the neural sheet with twice the stimulus frequency. The parametric excitation has two main characteristics: First, it provides a frequency selection by enforcing stable and unstable solutions dependent on the relation between $\omega_i = (\Omega_0^2 - v^2\triangle)^{1/2}$ and Ω. The unstable solutions are obtained for $\omega_i/2\Omega = k$, where $k = 1/2, 1, 3/2, \ldots$. Second, the parametric excitation causes a bistable situation for the relative phase between stimulus signal and the first temporal Fourier component of the first field mode. In contrast a linear driving term like K_3 causes a purely monostable situation which is not observed in the Kelso experiment. Thus the parametric excitation *must* be the dominant excitation.

In order to treat the system (17) analytically we perform a mode expansion

$$\psi_e(x,t) = \sum_{n=-1}^{1} \xi_n(t)\exp(inkx), \quad (19)$$

where $\xi_n(t) = \xi_{-n}^*(t)$ and the asterisk indicates the complex conjugate. The geometry of the brain, given by the dimension and the boundary conditions, is an open nontrivial question. Two geometries are proposed [5]: a closed sphere and a closed one-dimensional loop. Here we assume periodic boundaries of the neural sheet and only take standing waves into account. In our present one-dimensional description the first experimental order parameter state corresponds to the spatial mode with $n = 0$ in (19) and the second to $n = 1$. We make the following ansatz for the time-dependent amplitudes ξ_0 and ξ_1:

$$\xi_j = \sum_{m=0}^{2} \xi_j^{(m)}\exp(im\Omega t) + \mathrm{c.c.}, \qquad j = 0, 1, \quad (20)$$

where c.c. denotes the complex conjugate. The complex amplitude $\xi_j^{(m)}$ is slowly varying in time with respect to $2\pi/\Omega$ and higher harmonics are neglected. Following the lines in [2] we can investigate the dynamics of the amplitude and phase of $\xi_j^{(m)}$ separately and calculate their time-independent stationary solutions. The stability of these stationary solutions can be determined in dependence of the parameters. In the case of a strong parametric excitation of the neural sheet the relative phase between the first mode ξ_0 and the stimulus signal will show bistability or monostability depending on the time-independent stationary solutions of the amplitudes of $\xi_j^{(m)}$. This dependence can be explicitly calculated.

Numerical simulations of (17) yield the following behavior: Only standing waves are observed. In Fig. 2 the first and second rows present the pretransition situation at $\Omega = 0.31$ where ξ_0 (bold line) is in the unstable region of $k = 1/2$ and dominates oscillating with Ω in phase (first row) and in antiphase (second row). The stimulus signal (dotted line) is also plotted there. All higher modes are damped. Note that here the terms in phase and antiphase refer to the situation where the motor behavior is in phase or antiphase with respect to the stimulus signal. Because of possible fixed phase shifts between ξ_0 and the motor signal the field mode ξ_0 may be shifted with respect to the auditory stimulus. The temporal behavior of ξ_0 directly corresponds to the motor behavior in the case of the Kelso experiment, since the finger oscillator has been modeled as linearly driven by the motor areas in the brain which are localized such that ξ_0 is selected as the driving force. The third row shows the transition regime at $\Omega = 0.4$ where the second mode ξ_1 (slim line) reaches the unstable region $k = 1$ and comes up oscillating with 2Ω. Here the first mode ξ_0 performs a transition by π in the relative phase to the stimulus signal and gets damped via the cubic cross coupling. The bottom row shows the stationary situation in the postransition region at $\Omega = 0.47$ dominated by ξ_1. Here ξ_0 has a smaller amplitude and is monostable in the relative phase to the stimulus signal. The field parameters used for the numerical simulations are $\omega_0 = 0.15$, $\Omega_0 = 0.35$, $\tilde{\omega}_0 = 2.3$, $\epsilon = 0.5$, $A = 5 \times 10^{-3}$, $B = 0.4$, $\gamma_0 = 0.03$, $\gamma_1 = 0.8$, $C = 0.1$, $D_1 = D_2 = 0$. The extension of the neural sheet is $R_0 = 10$. Here the time unit corresponds to 20 msec and the space unit to 1 cm.

In our field equation we made simplifying assumptions about the boundaries, the distribution of fibers, and the spatial localization of the involved functional units. Towards a more realistic description an inhomogeneous distribution of the corticocortical fibers should be considered. Such an inhomogeneous distribution serves as a projection mechanism among cortical areas and undergoes changes during the growth of humans from child to adult. The spatial localization of functional units might be related to this development. Other units of the brain like the thalamus or the cerebellum were entirely neglected here and might be embedded within the neural sheet according to the here introduced notion of functional units. Cognitive aspects are involved in the conversion operations: The slope of the pulse-to-wave conversion changes with learning, the slope of the wave-to-pulse conversion changes with arousal.

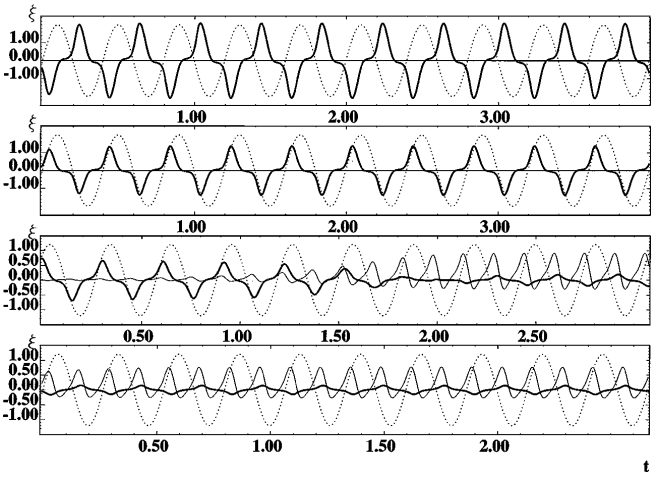

FIG. 2. The temporal behavior of the amplitudes of the field modes ξ_0 (bold line) and ξ_1 (slim line) and the external stimulus signal (dotted line) is plotted over the time t for different stimulus frequencies. The amplitudes are scaled in arbitrary units and the time in sec. See main text for details.

We gratefully acknowledge useful discussions with M. Bestehorn, R. Friedrich, and A. Fuchs. We wish to thank A. Schüz and P. Nunez for helpful comments about anatomy and physiology.

[1] H. Haken, *Synergetics: An Introduction* (Springer, Berlin, 1983), 3rd ed.
[2] V. K. Jirsa, R. Friedrich, H. Haken, and J. A. S. Kelso, Biol. Cybernet. **71**, 27–35 (1994).
[3] J. A. S. Kelso, S. L. Bressler, S. Buchanan, G. C. DeGuzman, M. Ding, A. Fuchs, and T. Holroyd, Phys. Lett. A **169**, 134–144 (1992).
[4] W. J. Freeman, Int. J. Bifurcation Chaos **2**, 451–482 (1992).
[5] P. L. Nunez, *Neocortical Dynamics and Human EEG Rhythms* (Oxford University Press, New York, 1995).
[6] M. Abeles, *Corticonics* (Cambridge University Press, Cambridge, England, 1991).
[7] R. Miller, Psychobiology **15**, 241–247 (1987).
[8] V. Braitenberg and A. Schüz, *Anatomy of the Cortex: Statistics and Geometry* (Springer, Berlin, 1991).
[9] P. L. Nunez, Math. Biosci. **21**, 279–297 (1974).
[10] V. K. Jirsa, R. Friedrich, and H. Haken, Physica (Amsterdam) **89D**, 100–122 (1995).